Biochimica et Biophysica Acta, 1099 (1992) 193–202

BBABIO 43572

The reaction center of Photosystem II studied with polarized fluorescence spectroscopy

Stefan L.S. Kwa, William R. Newell, Rienk van Grondelle and Jan P. Dekker

Department of Physics and Astronomy, Free University, Amsterdam (Netherlands)

(Received 3 July 1991)
(Revised manuscript received 31 October 1991)

Key words: Photosystem II; Reaction center; Polarized fluorescence; Linear dichroism

Low-temperature steady-state emission properties have been analyzed of Photosystem II reaction center (RC) complexes isolated from spinach CP47-RC complexes after a short Triton X-100 treatment and stabilization in *n*-dodecyl β,D-maltoside. Excitation spectra of the fluorescence anisotropy were detected at the maximum of the single fluorescence band at 683.5 nm and at the vibrational subband of the same emission at 742 nm. The Q_y transitions of the red-most absorbing pigment(s) showed positive anisotropy with a value of about 0.22. The value is lower than that of the theoretical maximum (0.4) and is explained by a combination of (1) vibrational depolarization effects and (2) by assuming that the red-most absorbing pigments arise from the low-exciton component of P680, that the exciton coupling breaks upon excitation, and that the angle between the monomer Q_y transitions of P680 is $48 \pm 10°$. The Q_x transitions of pheophytin showed negative anisotropy. This result, combined with the results obtained with linear dichroism spectroscopy, suggests that the spatial organization of the Q_x transitions of pheophytin matches the organization of the bacteriopheophytin residues in the bacterial reaction center. The spatial organization of the *y*-polarized transitions of pheophytin could be similar in both systems, although these transitions could also be tilted somewhat more towards the membrane plane in PS II. The data furthermore indicate that the accessory chlorophylls in PS II and in bacterial reaction centers have different average orientations, and suggest that at least some of the accessory chlorophylls in PS II have a pheophytin-like orientation.

Introduction

The photochemical reaction center of Photosystem II (PS II) consists of a structure comprising the so-called D1 and D2 proteins, cytochrome *b*-559 and the *psbI* gene product that resembles the well-known organization of the reaction center of photosynthetic purple bacteria [1]. Obvious similarities include the organization of the electron acceptor chain, where both systems use very similar quinone-iron complexes as ultimate acceptors [2], and a (bacterio)pheophytin residue as the primary electron acceptor. The pheophytin acceptors have been shown to be bound to both types of reaction center protein in comparable ways [3–6], with Q_x transitions almost in the plane of the membrane in vivo, and Q_y transitions at an angle of 45–65° [6].

In the bacterial system, the primary electron donor consists of a pair of exciton-coupled bacteriochlorophyll molecules. In PS II, however, the nature of primary electron donor P680 is not clear yet. Van Kan et al. [7] proposed a dimeric arrangement of chlorophyll with exciton bands at 679.5 and 683.5 nm and with an angle of about 60° between the Q_y transitions of the monomers. Braun et al. [8] also favored a dimeric arrangement, but with exciton bands at 679 and 669 nm and a configuration that resembles the bacterial special pair dimer. In order to explain the absence of pronounced red-shifts, the distance between the planes of the two chlorophyll molecules was proposed to be considerably larger in PS II. Tetenkin et al. [9] pointed out that excitonic interactions can take place among all porphyrin molecules of the complex, and that P680 could as well be a monomeric Chl molecule. The PS II reaction center contains more pigment than expected from the 4:2:1 stoichiometry of Chl : Pheo : Car of the bacterial system. A number of

Abbreviations: PS, Photosystem; P, primary donor; Chl, chlorophyll; Pheo, pheophytin; BChl, bacteriochlorophyll; BPheo, bacteriopheophytin; Car, carotenoid; Cyt, cytochrome; RC, reaction center; BisTris, 2-[bis(2-hydroxyethyl)amino]-2-hydroxymethylpropane-1,3-diol; LD, linear dichroism.

Correspondence: S.L.S. Kwa, Department of Physics and Astronomy, Free University, De Boelelaan 1081, 1081 HV Amsterdam, Netherlands.

recent reports point to a 6:2:2 stoichiometry [10–12], although some variability could occur depending on the specific isolation procedure used [13].

Information about the structural organization of the chlorophylls in the reaction center of PS II is relatively scarce. According to Van Kan et al. [7], the Q_y transitions of the two chlorophyll constituents of P680 are solely responsible for the observed absorption peak at 680–682 nm. This optical transition is expected to be oriented at a small angle with the plane of the membrane in vivo [6,14,15]. The accessory chlorophylls absorb around 670 nm [7], and do not show pronounced linear dichroism signals, except for a component peaking at 666 nm which is oriented almost perpendicular to the plane of the membrane [6].

We applied polarized fluorescence spectroscopy in order to obtain more information on the spatial arrangement of the pigments in the reaction center of PS II. Previously [16], we reported polarized excitation spectra of reaction centers prepared basically according to the original report of Nanba and Satoh [17]; the analysis, however, was complicated because the material exhibited several emission bands, of which the component peaking near 670 nm is suspected to be the result of destabilization by Triton X-100 [18]. In this contribution, we report polarized fluorescence spectra of carefully prepared and stabilized reaction centers that are characterized by a single emission band peaking around 683.5 nm. The results suggest that the spatial organization of the Q_x transitions of pheophytin and of the Q_y transition of the emitting chlorophyll species is in agreement with the organization of bacteriopheophytin and the primary electron donor in the bacterial reaction center.

Materials and Methods

CP47-D1-D2-Cyt*b*559 (CP47-RC) complexes were isolated from spinach using the non-ionic detergent *n*-dodecyl β,D-maltoside as described earlier [13] and used as starting material for the isolation of RC complexes with the detergent Triton X-100. The CP47-RC complexes were (at a concentration of about 1 mM Chl) diluted with 9 vol. of 2.5% Triton X-100 in BTT (20 mM BisTris, 20 mM NaCl, 10 mM $MgCl_2$, 1.5% taurine (pH 6.5)). After 15 min incubation, the material was applied to a Q-Sepharose column equilibrated with BTT + 0.2% Triton X-100. The column was washed with one column volume BTT + 0.2% Triton X-100, about 10 column volumes BTT + 0.03% dodecyl maltoside, and one column volume BTT + 20 mM $MgSO_4$ + 0.03% dodecyl maltoside, after which the RC complex was eluted with BTT + 100 mM $MgSO_4$ ± 0.03% dodecyl maltoside, frozen and stored at −70°C until further use. Alternatively, RC complexes were isolated following the above method, except that taurine was omitted in all buffers. All procedures were carried out at 4°C, and especially during exposure to Triton X-100 care was taken to avoid illumination.

For 77 K and 4 K measurements, the samples were diluted in BTT + 0.03% (w/v) dodecyl maltoside + 70% (w/v) glycerol in a 1.0 × 1.0 cm Perspex cuvette and cooled to 77 K in a nitrogen reservoir cryostat (Oxford) or to 4 K in a helium flow cryostat (Oxford). Absorption spectra were measured with a Cary 219 spectrophotometer and linear dichroism spectra were measured as described earlier [15] with a modified Cary 61 spectropolarimeter. Orientation of the particles was achieved by squeezing a 1.25 × 1.25 cm polymerized polyacrylamide gel simultaneously in two perpendicular directions into a 1.0 × 1.0 cm cuvette, allowing it to expand in the third dimension. Linear dichroism is defined here as the difference between absorption of light polarized parallel and perpendicular to this third dimension. The final composition of the gel was 66% (w/v) glycerol, 14.5% (w/v) acrylamide, 0.5% (w/v) bisacrylamide in BTT + 0.03% dodecyl maltoside, polymerized with 0.01% (w/v) ammonium persulphate and 0.03% (v/v) TEMED.

Fluorescence was measured on a home-built fluorimeter with excitation and emission beams at right angles. The excitation source was a 150 W tungsten halogen lamp equipped with a 1/8 m monochromator (Oriel 77250) and a polarizer. The emission light was passed through an OG550 filter, a polarizer and a 1/8 m double monochromator (Oriel 77274), and detected with a S-20 photomultiplier cooled to −20°C, which was used in photon counting mode. Distortion of excitation and emission spectra due to inner filter effect and self-absorption, respectively, was minimized by using an optical absorbance of less than 0.05 cm^{-1} in the red absorption peak of the sample. For anisotropy measurements, an absorbance of 0.3 cm^{-1} was used. Emission spectra were corrected after measurement of the sensitivity curve of the detection system with a 1000 W Quartz Halogen calibration lamp (Eppley, G.E. DWX). The wavelength calibration of the equipment described here was checked with the absorption lines of a didymium oxide filter. The fluorescence anisotropy, r, and fluorescence polarization, P, are defined as

$$r \equiv \frac{I_{\parallel} - I_{\perp}}{I_{\parallel} + 2I_{\perp}} \text{ and } P \equiv \frac{I_{\parallel} - I_{\perp}}{I_{\parallel} + I_{\perp}} \quad (1)$$

where $I_{\parallel}$ and $I_{\perp}$ are the intensities of the emission beam with polarization direction oriented parallel and perpendicular, respectively, to the polarization direction of the excitation light [19]. The anisotropy depends on the angle θ between absorption and emission dipole moment in the following way [19]:

$$r = \tfrac{1}{5}(3\cos^2\theta - 1) \quad (2)$$

Anisotropy, r, can vary between $+2/5$ ($\theta = 0°$) and $-1/5$ ($\theta = 90°$). If more than one absorption and/or emission dipole moment is involved, expression (2) becomes

$$r = \sum_{i,j} f_{ij} r_{ij} = \sum_{i,j} f_{ij} \cdot \tfrac{1}{5}\left(3\cos^2\theta_{ij} - 1\right) \qquad (3)$$

where f_{ij} is the fractional contribution to the fluorescence of a specific absorption and emission dipole moment couple i and j with an angle θ_{ij} [20].

Angles between transition moments in the reaction center of *Rps. viridis* were calculated from the crystal structure coordinates by Deisenhofer et al. [21]. The coordinates were obtained from the Brookhaven Protein Data Bank. The x- and y-axes in BChl and BPheo were defined as the line through nitrogen atoms N_A and N_C and the line through N_B and N_D and the angles were chosen between 0° and 90°.

Results

We isolated the reaction center of PS II by a modified method by which the time of exposure to the detergent Triton X-100 could be reduced drastically from overnight to about 1 h. Fig. 1 (drawn line) shows the 77 K absorption spectrum, which appears almost identical to the one reported earlier by Van Kan et al. [7] on longer exposed (but carefully treated) samples, with sharp peaks near 679 and 671 nm of $Q_{y(0\text{-}0)}$ transitions of Chl *a* and Pheo *a*, a pronounced 542 nm peak originating from the $Q_{x(0\text{-}0)}$ transition of Pheo *a* and a characteristic structure in the β-carotene absorption region with peaks at 505 and 489 nm. The spectrum appeared to be dependent on the presence of taurine in the isolation buffers. Without taurine a smaller amplitude of the carotenoid absorption was

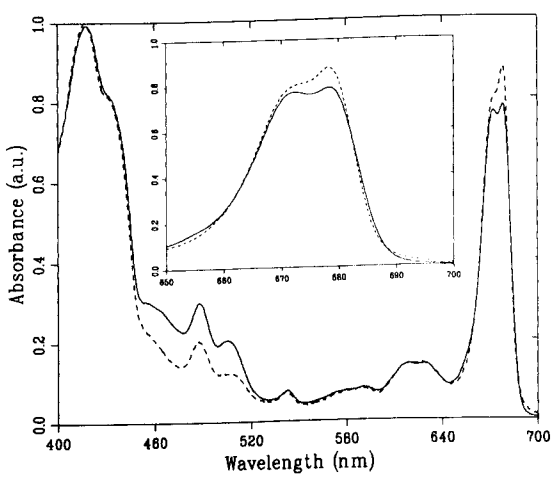

Fig. 1. 77 K absorbance spectra of PS II RC complexes in the presence (———) or absence (- - - - - -) of taurine. Both spectra were normalized at 415 nm. Inset: enlargement of the $Q_{y(0\text{-}0)}$ absorption region (650–700 nm).

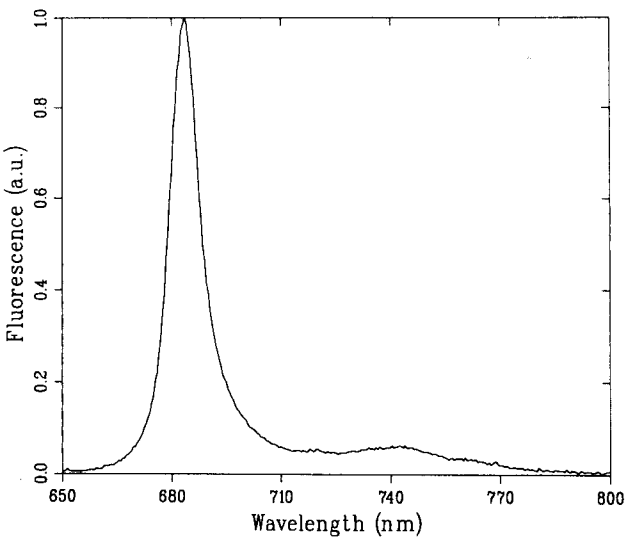

Fig. 2. 77 K fluorescence emission spectrum of PS II RC (+taurine) with excitation at 436 nm. The spectral bandwidth was 15 nm for excitation and 1.5 nm for detection.

observed, although the relative amplitudes of the in-plane and out-plane transitions [6,13,15], peaking at 506 and 489 nm, respectively, have not changed. The shape of the absorbance spectrum around 675 nm also appeared somewhat different (Fig. 1, dashed line).

The 77 K fluorescence emission spectrum shows a single peak at 683.5 nm (Fig. 2) without apparent shoulders, in accordance with data reported by other investigators (see, e.g., Ref. 22). The absence of a clear shoulder or peak at 672 nm (observed in partially destabilized samples – see, e.g., Refs. 16, 18, 23, 24) is an indication that unconnected pigments are not contributing to the steady-state emission. The shape of the spectrum appeared to be independent of excitation wavelength (417, 436, 489 or 620 nm). In addition, the shape of the 77 K fluorescence excitation spectrum (Fig. 3a) was independent of detection wavelength (678, 684, 692 and 742 nm), suggesting that good equilibration of excitation energy before fluorescence, as observed in these steady-state spectra, occurs. By comparing the shapes of excitation and absorbance spectra (Figs. 3a and 1, drawn line), the transfer efficiency of β-Car to Chl *a* was estimated to be about 30% of the efficiency of Chl *a* or Pheo *a* to Chl *a*. This low value is in line with earlier observations by Van Dorssen et al. [14]. The absence of taurine did not result in a significant change of the fluorescence emission spectrum (not shown), although the quantum yield seemed to be considerably lower.

Fig. 3b presents the anisotropy of the fluorescence excitation spectra (anisotropy spectra) at 77 K, and compares these spectra with the linear dichroism (LD) spectrum of this preparation. For measuring the LD spectrum, we used similar orientation methods as used earlier by Van Dorssen et al. [14], Breton [6] and

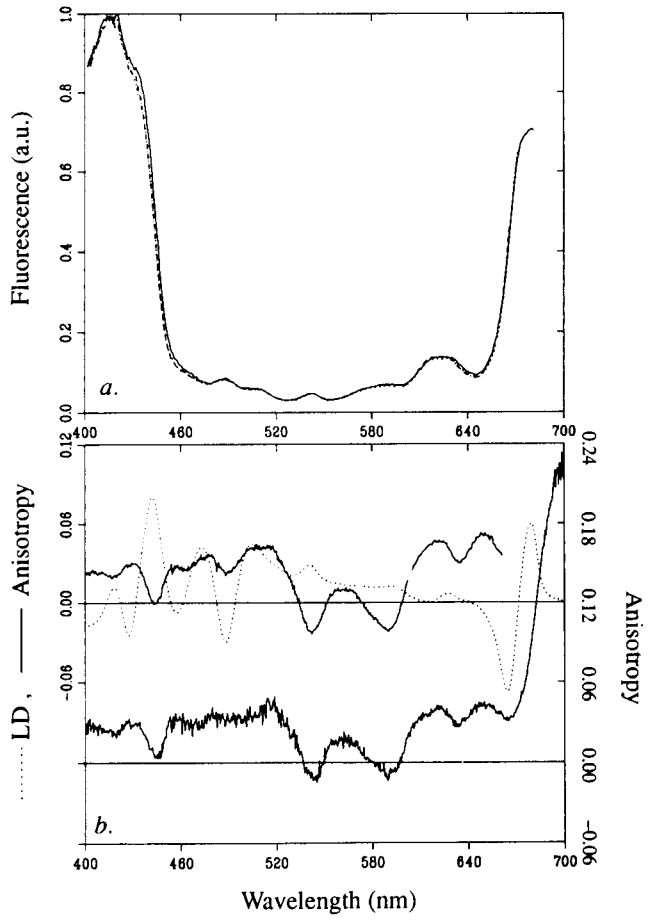

Fig. 3. (a) 77 K fluorescence excitation spectra of PS II RC (+taurine). Detection was at 692 nm (———), 684 nm (· · · · · ·) and 678 nm (- - - - -). The spectral bandwidth was 6 nm for excitation and detection. (b) 77 K fluorescence excitation spectra of the anisotropy with detection at 684 nm (upper curve) and 742 nm (lower curve), and 77 K linear dichroism spectrum of PS II RC (+taurine, dotted line). The anisotropy spectra were recorded with a spectral bandwidth of 6 nm for excitation and 12 nm for detection, and the LD spectrum with a resolution of 2 nm.

Newell et al. [15] and we found a very similar spectrum (Fig. 3b, dotted line). Van Dorssen et al. and Breton concluded that the directions of the complex which are in vivo parallel to the membrane plane orient in the gel perpendicular to the squeezing direction, i.e., give rise to a positive LD. Thus, the positive peak at 680 nm indicates that the $Q_{y(0\text{-}0)}$ transition(s) of the red-most absorbing pigment(s) are more or less oriented in the plane of the membrane. The LD spectrum further shows that the Q_x transition of pheophytin at 543 nm also is oriented rather parallel to the membrane plane. If the 680 nm transition originates from the primary electron donor [7], then both orientations with respect to the membrane plane are similar to the orientations of the corresponding transitions in the bacterial reaction center [21].

We recorded the anisotropy spectra (Fig. 3b, drawn lines) in the emission maximum at 683.5 nm and in the vibrational subband at 742 nm (see Fig. 2); the $Q_{y(0\text{-}0)}$ absorption region and the Pheo *a* Q_x region were also analyzed with increased spectral resolution of the excitation light (Fig. 4). The anisotropy spectra in Fig. 3b are almost identical, confirming that the emission dipole moments of the main and subband transitions have parallel orientations. The anisotropy spectra have the following general characteristics: (1) above 685 nm, the anisotropy value is relatively high (0.22 ± 0.02), but significantly lower than the theoretical maximum value of +0.4 (see Eqn. 2); (2) below 685 nm, the anisotropy value gradually decreases to a minimum of about +0.03 at 666 nm; (3) a second minimum of about the same value is observed around 633 nm; (4) minima with negative anisotropy values are observed at Q_x region of Chl *a* and Pheo *a* around 590 and 542 nm, respectively; (5) surprisingly, small changes in anisotropy are observed when scanning the carotenoid absorption re-

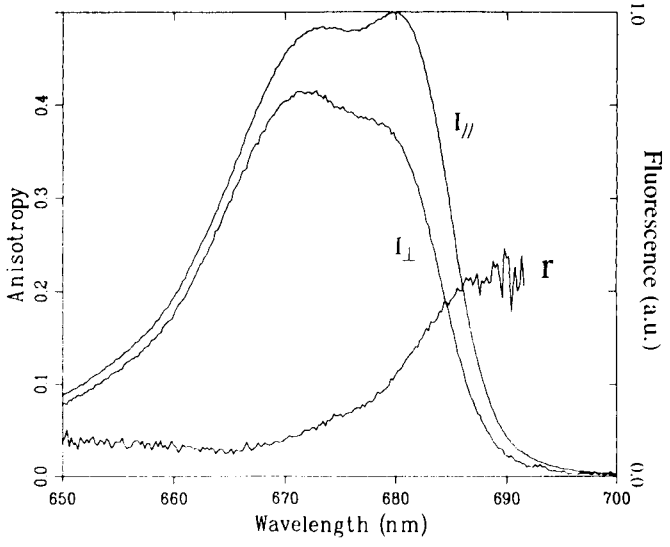

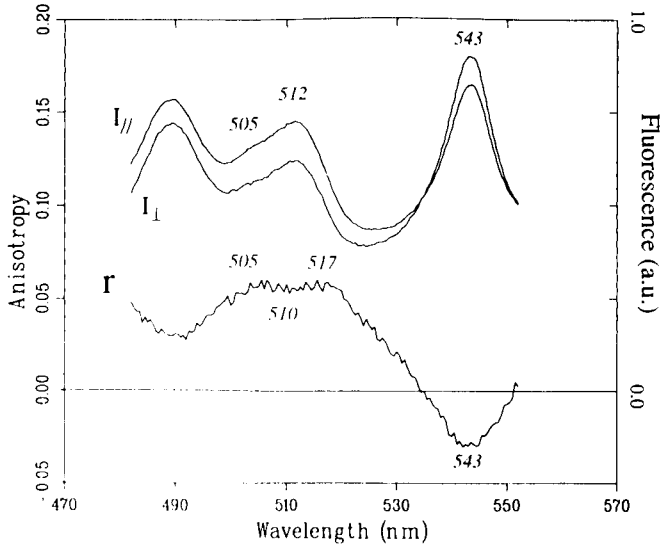

Fig. 4. (a) $Q_{y(0\text{-}0)}$ region of 77 K fluorescence excitation spectra $I_{\parallel}$ and $I_{\perp}$, and the anisotropy of PS II RC (+taurine) detected at 742 nm. The spectral bandwidth was 1.5 nm for excitation and 12 nm for detection. (b) as (a), but excitation in the Pheo *a* Q_x region and detection at 684 nm.

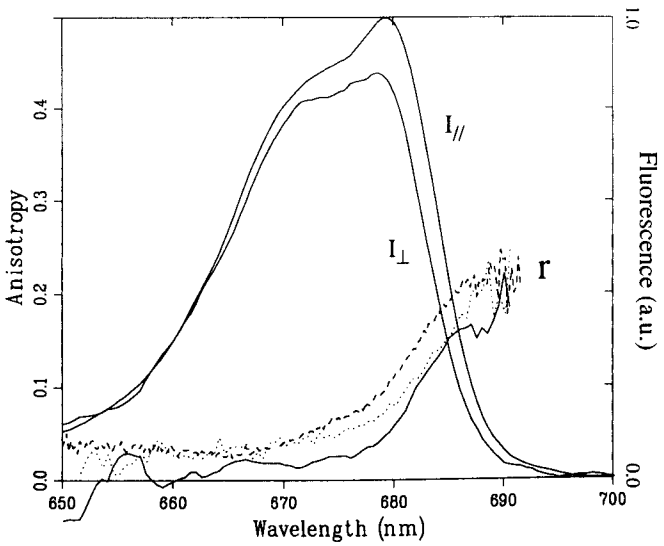

Fig. 5. Spectra of PS II RC: (———) 4 K fluorescence excitation spectra $I_{\parallel}$ and $I_{\perp}$, and the anisotropy (−taurine); (· · · · · ·) 77 K anisotropy spectrum (−taurine); (- - - - -) 77 K anisotropy spectrum (+taurine, see Fig. 4a). The detection wavelength was 742 nm. The spectra of PS II RC in the absence of taurine were recorded with a spectral bandwidth of 3 nm for excitation and 12 nm for detection.

gion; (6) the anisotropy values detected at 742 nm are 15–25% smaller than those detected at 684 nm.

The 77 K anisotropy spectrum in Fig. 4a appeared to be the same for different preparations and did not change significantly in the absence of taurine, or upon cooling down to 4 K (Fig. 5). The latter finding indicates that there is one major energy level from which excited states return to the ground state at 77 K. The possibility can, however, not be excluded that this energy level is degenerate, i.e., that there is more than one transition responsible for emission.

Discussion

The anisotropy spectra reported in this contribution extend the information on the orientation of pigments in the reaction center of PS II. Whereas the earlier reported (and here confirmed) linear dichroism data [6,14,15] give, in this particular case, information on the orientation with respect to the plane of the membrane in vivo, the anisotropy spectra give information on the orientation with respect to the emitting dipole moment(s). That both orientations yield additional information becomes immediately clear when examining the red-most absorbing pigments (the best candidates for being responsible for the steady-state emission) and the Q_x transition of pheophytin, which both show parallel orientations with respect to the membrane plane, but almost perpendicular orientations with respect to each other.

Qualitatively, the experimentally observed orientations of the Q_y transitions of the red-most absorbing pigments and of the Q_x transitions of pheophytin are expected if (1) the red-most absorbing pigments arise from the primary electron donor P680 and if (2) these pigments have similar orientations in the reaction center of PS II and in the bacterial reaction center. Thus, the average orientations in PS II of the Q_x transition of pheophytin and of the Q_y transition of P680 resembles the bacterial organization, and confirms the similarity of the primary photochemical reactants of both systems [1].

Anisotropy of the bacterial reaction center

In order to determine more quantitatively to which extent it is possible to describe our PS II data with the bacterial organization, we have calculated angles between transition moments in the reaction center from *Rps. viridis*, using the coordinates from the crystal structure by Deisenhofer et al. [21]. These angles are shown in Table I and are in good agreement with absorbance difference polarization data of isolated reaction centers of *Rps. viridis* in solution [25]. Using Eqn. (2), we obtained the corresponding anisotropy value, r, for every angle (Table I).

The uncertainty of the bandpositions of the different PS II pigments, the unknown identity of the emitting pigment(s), and the unknown extent of excitonic interactions between the pigments, however, complicate a direct comparison of the r-values in Table I with the PS II data. Therefore, we consider in Table I several possible emission dipole moments: (1) the lowest exciton transition of P (the sum of the monomer Q_y transitions), in case of emission by the red-most exciton transition, (2) the monomer Q_y transitions of P, in case of a breaking of the exciton interaction upon excitation [26], and (3) the Q_y transitions of BPheo.

It appears from Table I that the six emission transitions listed can roughly be divided into two groups. The mean r-value ($\bar{r}$) of two homologue pigments on the L- and M-subunit are similar for the $PQ_yL + PQ_yM$, PQ_yL and PQ_yM transitions (group A) and for the $BPheoQ_yL$, $BPheoQ_yM$ and $PQ_yL - PQ_yM$ transitions (group B).

Limiting anisotropy

The value of the anisotropy maximum above 685 nm appeared to be about +0.22 in the PS II RC particles at 77 K or 4 K (Figs. 4a and 5). This value is considerably lower than the theoretical maximum (+0.40). The lower value is not a result of imperfections of our equipment: for several other systems, such as the B820 subunit of the core-antenna of photosynthetic purple bacteria, a value very close to the theoretical maximum was observed [27]. Increasing the spectral resolution did not change the value of the limiting anisotropy. Therefore, the lower value is real, and is due to intrin-

TABLE I

Transition moment angles

Angles θ between transition moments in the reaction center from *Rps. viridis*, calculated from the coordinates of the crystal structure as given by Deisenhofer et al. [21]. Transition moments, represented by vectors, are denoted by pigment species (bacteriochlorophyll from P, voyeur Bchl or Bpheo), transition (Q_y or Q_x) and subunit to which the pigment is bound to (L or M). The vector sum or difference of the two Q_y transitions of P are notated as PQ_yL+PQ_yM or PQ_yL-PQ_yM, respectively. Expected anisotropy values (r) are calculated using Eqn. 2. Mean anisotropy values ($\bar{r}$) are given in the case of more than one absorption transition.

	Group A									Group B								
	PQ_yL+PQ_yM			PQ_yL			PQ_yM			Bpheo Q_yL			Bpheo Q_yM			PQ_yL-PQ_yM		
	θ	r	$\bar{r}$	θ	r	$\bar{r}$	θ	r	$\bar{r}$	θ	r	$\bar{r}$	θ	r	$\bar{r}$	θ	r	$\bar{r}$
PQ_yL+PQ_yM	0°	*+0.4*	+0.4	19.3°	*+0.33*	+0.33	19.3°	*+0.33*	+0.33	72.5°	*−0.15*	−0.15	69.8°	*−0.13*	−0.13	90°	*−0.2*	−0.2
PQ_yL	–			0°	*+0.4*	+0.28	38.6°	*+0.17*	+0.28	89.6°	*−0.20*	−0.10	53.6°	*+0.01*	−0.09	–		
PQ_yM	–			38.6°	*+0.17*		0°	*+0.4*		54.9°	*0.00*		86.7°	*−0.20*		–		
BPheo Q_yL	72.5°	*−0.15*	−0.14	89.6°	*−0.20*	−0.09	54.9°	*0.00*	−0.10	0°	*+0.4*	+0.16	64.4°	*−0.09*	+0.16	28.4°	*+0.26*	+0.23
BPheo Q_yM	69.8°	*−0.13*		53.6°	*+0.01*		86.7°	*−0.20*		64.5°	*−0.09*		0°	*+0.4*		36.0°	*+0.19*	
BChl Q_yL	29.3°	*+0.26*	+0.28	46.6°	*+0.08*	+0.23	16.5°	*+0.35*	+0.25	58.3°	*−0.03*	−0.11	80.9°	*−0.19*	−0.12	65.7°	*−0.10*	−0.12
BChl Q_yM	23.5°	*+0.30*		12.5°	*+0.37*		41.1°	*+0.14*		84.3°	*−0.19*		61.0°	*−0.06*		70.4°	*−0.13*	
PQ_yL-PQ_yM	90°	*−0.2*	−0.2	70.7°	*−0.13*	−0.13	70.7°	*−0.13*	−0.13	28.4°	*+0.26*	+0.26	36.0°	*+0.19*	+0.19	0°	*+0.4*	+0.4
PQ_xL	71.6°	*−0.14*	−0.14	89.1°	*−0.20*	−0.09	52.4°	*+0.02*	−0.09	16.9°	*+0.35*	+0.22	51.9°	*+0.03*	+0.17	19.0°	*+0.34*	+0.33
PQ_xM	71.4°	*−0.14*		52.3°	*+0.02*		89.4°	*−0.20*		46.8°	*+0.08*		21.7°	*+0.32*		20.0°	*+0.33*	
BPheo Q_xL	72.9°	*−0.15*	−0.11	77.7°	*−0.17*	−0.11	70.0°	*−0.13*	−0.13	85.1°	*−0.20*	−0.15	60.0°	*−0.05*	−0.12	78.8°	*−0.18*	−0.17
BPheo Q_xM	62.4°	*−0.07*		58.9°	*−0.04*		69.1°	*−0.12*		67.1°	*−0.11*		87.2°	*−0.20*		75.9°	*−0.17*	
BChl Q_xL	66.1°	*−0.10*	−0.12	60.1°	*−0.05*	−0.12	74.5°	*−0.16*	−0.13	82.9°	*−0.19*	−0.04	34.3°	*+0.21*	+0.03	69.4°	*−0.13*	−0.13
BChl Q_xM	71.7°	*−0.14*		79.3°	*−0.18*		66.0°	*−0.10*		44.3°	*+0.11*		74.8°	*−0.16*		70.5°	*−0.13*	

sic spectroscopic properties of Chl *a* and/or to the structure of the PS II reaction center.

Van Gurp et al. [20] found that the limiting steady-state fluorescence anisotropy for Chl *a* at low temperatures is 0.365 upon excitation in the $Q_{y(0\text{-}0)}$ absorption band and detection in the main emission band. The theoretical maximum anisotropy value (0.4) was not reached, which was explained by internal motions of the molecule, causing depolarization on the picosecond timescale. At 4°C, the maximum anisotropy value was found to be 21% lower upon detection in the vibrational subband instead of the main emission band. Using this value for lower temperatures, the maximum anisotropy for Chl *a* with detection in the vibrational subband can be calculated to be +0.29. This depolarization effect can be explained by a greater uncertainty in the transition direction of the vibrational subband. A similar effect is seen in anisotropy spectra from the PS II reaction center (Fig. 3b), with about the same amplitude difference (15–25%).

Thus, in order to correct for this depolarization effect, the *r*-value of $+0.22 \pm 0.02$ for the maximum anisotropy of the PS II RC should be rescaled with a factor of maximally 0.4/0.29. This means that the maximum, corrected anisotropy for the PS II RC would be $0.22 \times (0.4/0.29) = 0.30$.

Red-most absorbing pigments

The rescaled maximum anisotropy of the PS II RC (0.30) is significantly less than 0.4, the limiting anisotropy value. This implies that there exist more than one red-most absorbing pigments and/or emission transitions, which are not exactly, but approximately parallel.

Several workers have proposed assignments of bandpositions of the pigments. In the view of Van Kan et al. [7], P680 is the red-most absorbing species with exciton bands at 683.6 and 679.6 nm and therefore expected to be responsible for most of the steady-state emission. The Pheo *a* molecules at 676.5 nm could, however, also contribute to the emission if Pheo *a* has a larger Stokes shift than P680. In the view of Braun et al. [8], the exciton bands of P680 are placed much further apart at 680 and 668 nm. Pheo *a* and the accessory Chl *a* are positioned around 671–673 nm, leaving P680 as the only possible emitter. In the view of Tang et al. [28], both P680 and the photoactive pheophytin absorb at 681.5 nm, due to which both should be considered as possible emitters.

We compared our measured anisotropy values with values generated using bandpositions given by Refs. 7 and 8, with either group A, group B or both groups as emitting species (Table I).

With the band positions proposed by Van Kan et al. [7], the anisotropy with either group A or group B transitions as emitters is expected to be large and opposite of sign at the exciton band positions at 683.6 and 679.6 nm, since the two exciton transitions of a dimer are always perpendicular. Our measured anisotropy spectra do not show this behavior (Fig. 4a). The anisotropy is most positive above 686 nm, but stays positive at 679 nm. A reason for not observing negative anisotropy at 679 nm could be provided by a third band with a positive anisotropy. However, the nearest band in the assignment of Ref. 7 is the Pheo *a* band at 676.5 nm, which shows too little overlap with the 679.6 nm band (5–6 nm bandwidths at 10 K [7]) to compensate the negative anisotropy sufficiently.

If both group A and group B transitions contribute to the emission, the *r*-values for each absorbing species are averaged over group A and group B emitters. This generates the following *r*-values (by averaging all $\bar{r}$-values in a row in Table I, equal weights for all emission transitions): +0.10 around 683.6 nm ($PQ_yL + PQ_yM$), +0.07 around 679.6 nm ($PQ_yL - PQ_yM$) and +0.03 around 676.5 nm ($BPheoQ_y$). Here, the experimentally determined maximum *r*-value of +0.22 (or +0.30 after rescaling) is not reached. In fact, it is not possible to reach a large positive anisotropy with two perpendicular emitters. Putting more weight onto the group A emission leads to a higher calculated *r*-value around 683.6 nm, but lowers the value at 679.6 nm to negative values, which is not observed in our spectra (Figs. 4a and 5). We conclude that our anisotropy spectra cannot sufficiently be described with the band assignments of Van Kan et al. [7].

The inconsistency may be solved by placing the dimer bands much further apart, as in the assignment of Braun et al. [8]. The exciton transition responsible for the absorption above 680 nm, however, cannot be solely responsible for the emission, because in this case an anisotropy value of +0.4 is expected. This could suggest that the two *individual* Q_y *transitions* of the chlorophylls in P680 define the emission dipole moment. Similar suggestions have been proposed to explain the low polarization value observed in exciton-coupled bacterial light-harvesting systems [26,27]. Using the bacterial pigment organization (Table I) an *r*-value of 0.33 is found, which is similar to our rescaled value of 0.30. Thus, the angle between the Q_y transitions of P680 in PS II ($48 \pm 10°$) would be comparable to the situation in the bacterial reaction center (39°). The assignments of Braun et al. [8], however, do not explain the steep descent in the anisotropy from 686 down to 680 nm, since only one band is assumed around 680 nm. This descent can only be explained by one or more extra bands in the 678–682 nm absorption region, e.g., the Q_y transition of (photoactive) Pheo *a*, proposed by Tang et al. [28] to absorb above 680 nm, and/or the Q_y transitions of another (but monomeric) Chl *a* (see below).

As discussed above, the rescaled value of the anisotropy above 685 nm can be well explained by assuming a 'bacterial-RC'-like special pair organization. If, however, pheophytin emission would to some extent contribute to the observed emission spectrum, the situation could change (if the Q_y transitions of Pheo and of the special pair are not parallel, as in *Rps. viridis*). The fact that the maximum anisotropy values are the same at 77 K and 4 K suggests that the relative extent of the eventual pheophytin contribution to the emission must be the same at both temperatures. In addition, the shapes of the excitation spectra and the anisotropy spectra are independent of detection wavelength (683.5 or 742 nm), which means that the eventual pheophytin contribution must also be the same at both emission wavelengths. Taken together, it seems to be unlikely that pheophytin contributes significantly to the steady-state emission.

Summarizing, the available data suggest that (1) the red-most absorbing species is the low-exciton component of P680 [7], (2) the exciton coupling in P680 breaks upon excitation, and (3) the angle between the Chl *a* Q_y transitions contributing to P680 ($48 \pm 10°$) is about the same as in the bacterial reaction center (39°). The distance between the planes of the two porphyrin rings, however, should be at least 10 Å to account for the relatively small redshift [8].

Pheophytin

The polarized excitation spectrum of Pheo *a* in castor oil [29] shows an S-shape with a positive peak around 509 nm and a negative peak around 544 nm, which can be assigned to a *y*-polarized transition and the Q_x transition, respectively [30]. Assuming these transitions to be parallel or perpendicular, respectively, with the $Q_{y(0\text{-}0)}$ emission dipole moment, limiting polarization (or anisotropy) values are expected. However, values (here converted into anisotropy values) of $r = +0.08$ (509 nm) and $r = -0.01$ (544 nm) were reported. Apparently, internal molecular motion and strong overlap of bands occur in Pheo *a*. Also depolarization by Brownian motion cannot be ruled out at room temperature.

Previously, we reported fluorescence polarization spectra of PS II RC complexes in the presence of 0.20% (w/v) Triton X-100 [16], in which case the energy transfer between the pigments is drastically reduced [28]. A considerable amount of 674 nm emission was observed. The 77 K excitation spectrum of this emission clearly showed Pheo bands of the *y*-polarized and the Q_x transition at 509 and 540 nm, respectively, and the polarization spectrum showed the characteristic S-shape as in the Pheo *a* spectrum by Goedheer [29] peaking at 513 nm ($r = +0.06$) and 540 nm ($r = -0.07$). Therefore, we consider this spectrum to be dominated by the polarization or anisotropy of disconnected Pheo *a*. The slightly higher amplitude of the S-shape in this spectrum can be explained by the absence of Brownian motion in this case.

The RC anisotropy spectrum presented here also shows an S-shape (Figs. 3b and 4b), but with an amplitude smaller than for disconnected Pheo *a*. The peak values were found at 505–517 nm ($r = +0.05$) and 543 nm ($r = -0.03$). In the excitation spectrum (Fig. 4b) Pheo *a* peaks are observed at 512 and 543 nm and a β-carotene peak at 505 nm. Note that the S-shape and the Pheo *a* peaks in the anisotropy and excitation spectra are 3–4 nm red shifted with respect to the positions in the spectra from disconnected Pheo *a*.

The positive anisotropy at 517 nm may be ascribed to the *y*-polarized Pheo transition, and the positive anisotropy at 505 nm to carotene (the 4–5 nm redshift of the positive anisotropy peak compared to the approx. 510 nm peak in the excitation spectrum is also observed in disconnected and in vitro Pheo *a* [16,29]). This would mean that the average *y*-polarized Pheo transition is tilted somewhat towards the emission dipoles, and suggests that the Pheo Q_y transitions do not make such a large angle with the membrane plane as in the bacterial system, because the emitting dipoles are oriented preferentially parallel to the membrane plane.

Alternatively, the broad carotenoid peak could be solely responsible for the positive anisotropy between 500 and 520 nm and the *y*-polarized Pheo transition for the negative dip at 512 nm (Fig. 4b). This interpretation is similar to the interpretation of LD spectra by Breton [6], who suggested that the *y*-polarized Pheo transition gives a negative contribution around 512 nm. This would mean a non-parallel orientation of the Pheo Q_y transition with the emission dipole moments, and an orientation out of the membrane plane, as in the bacterial reaction center. This interpretation, however, also implies that another pigment at 676 nm should compensate for the negative anisotropy of the Q_y transition of Pheo *a*, because the observed value at 676 nm is about +0.07 (Fig. 4a).

Accessory chlorophyll

The Q_y transitions of accessory Chl *a* absorbing at 670 nm give rise to a very small positive anisotropy signal with a minimum around 666 nm (Fig. 4a), which means that these transitions are not parallel with the emission/red-most absorbing transitions. This is consistent with the LD-spectrum (Fig. 3b), where Chl a Q_y transitions give rise to a negative LD with a minimum around 666 nm, contrasting the positive LD of the red-most absorbing pigments. This situation differs from that of the bacterial reaction center, where the Q_y transitions of all four BChl molecules are approximately parallel, and give rise to positive anisotropy (Table I) and LD values [31]. This suggests that in PS

II at least some of the accessory chlorophylls have very different orientations than the accessory chlorophylls in the bacterial reaction center. In fact, some of the accessory chlorophylls could be oriented in similar ways as the BPheo residues in the bacterial RC.

EPR data from PS II membranes and D1/D2/Cyt*b*559 particles [32,33] indicated that the ring system of the flash-induced Chl-triplet makes a small angle with the plane of the membrane, and thus is oriented in about the same way as the accessory chlorophylls in the bacterial RC. This triplet originates from a Chl in PS II and was suggested to arise from P680 [33]. Equivalents of the special pair porphyrins were thought to be present in PS II, but not related to P680 [33]. Our finding that the Q_y transitions of the emitting species are oriented *similarly* as those of the special pair in the bacterial reaction center does not have to be in disagreement with these suggestions, because (1) our data only give information on the orientations of the Q_y transitions of the pigments and very little on the orientations of the Q_x transitions (other than that the average Q_x transition of *all* chlorophylls makes a relatively large angle with the emitting dipoles, in view of the negative features in the anisotropy spectra (Fig. 3b) around 590 nm) and (2) the angles between the Q_y transitions of the special pair and accessory Chl molecules are small in the bacterial system. Obviously, the chlorophyll responsible for the parallel triplet cannot be the only Chl absorbing in the 680 nm region, in view of the low-temperature absorption spectrum (Ref. 7, Fig. 1). Also, the low-exciton transition of the special-pair-like dimer most likely absorbs in this region. In fact, the anisotropy data in our contribution are most easily explained by assuming that the special-pair molecules are responsible for the steady-state emission, and that the Chl responsible for the triplet causes depolarization at 680 nm (possibly together with a Pheo absorbing in this region as proposed in Ref. 28). Which of the components really is equivalent to P680 is still a matter of debate; the triplet state could, for instance, be rapidly transferred from the special pair molecules to the accessory Chl, with preservation of the typical spin-polarized character.

Carotenoid

A large oscillating carotenoid LD signal has been observed in reaction centers and larger PS II particles (Fig. 3b and Refs. 6, 14, 15, 34–37). Van Dorssen et al. [13] and Breton [6] concluded that the carotenoid transitions at 442, 474 and 506 nm are oriented parallel to the membrane plane in vivo, while the transitions at 458 and 490 nm are oriented out of this plane. So the angle between the 'in plane' and 'out of plane' transitions is close to 90°. The anisotropy spectrum does exhibit only a small oscillating carotenoid signal. This can only in part be due to diminished carotene-to-chlorophyll exciton transfer, because the carotene transitions are clearly visible in the excitation spectrum (Fig. 3a). It therefore means that the average direction of the emission dipole moments can not be oriented exactly in the membrane plane (in that case the anisotropy of the out of plane carotenoid transitions would be strongly negative), but must be tilted slightly out of this plane. This is consistent with the interpretation that in PS II the low exciton band of P680 is parallel with the membrane plane and that the separate Q_y transitions, which make small angles (approx. 20–25°) with the exciton band and the membrane plane (as in the bacterial reaction center), are responsible for emission.

Conclusions

To summarize our results, we present in Fig. 6 a model which visualizes the angles between the dipole moments and which is consistent with the fluorescence data and the LD measurements (note that the distances are arbitrary and that the direction of the arrows can also be inverted). The Q_y bands of the P680 dimer (PQ_y1 and PQ_y2) are each tilted slightly out of the plane of the membrane, while their sum vector ($PQ_y1 + PQ_y2$, the low exciton component) is oriented

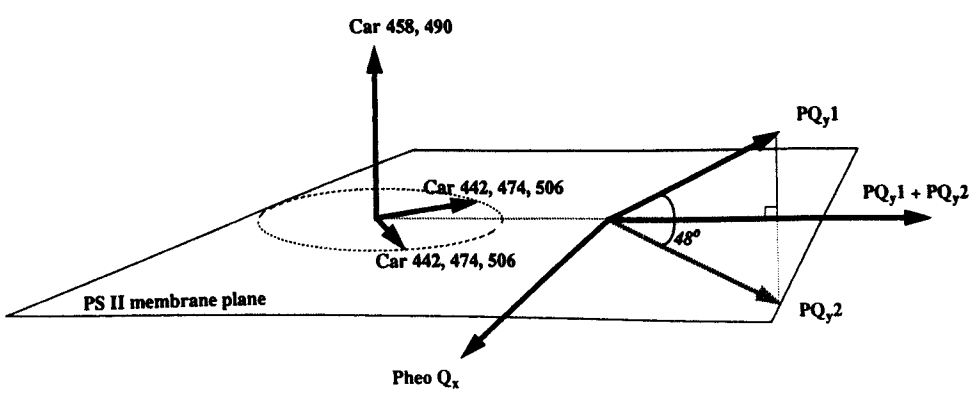

Fig. 6. Model of PS II RC, visualizing the angles between the dipole moments. Indicated are the Q_y bands of the P680 dimer (PQ_y1 and PQ_y2) the low exciton component ($PQ_y1 + PQ_y2$), Pheo Q_x, the carotenoid transitions at 458 nm and 490 (Car 458, 490) and at 442, 474 and 506 nm (Car 442, 474, 506).

in the plane of the membrane. The Pheo Q_x transition is at right angles to the P680 transitions, parallel to the membrane plane. The carotenoid transitions at 458 and 490 nm are oriented parallel to the membrane normal, while the transitions at 442, 474 and 506 nm are parallel to the membrane plane. The orientation of the latter transitions in the membrane plane can not be deduced very precisely, but the angle with the monomer Q_y bands of P680 should be about 55° or slightly smaller, leaving two possibilities, both of which are shown in Fig. 6.

Acknowledgements

We are most grateful to Mrs. Ineke Vlaanderen for expert technical assistance in the isolation of the PS II RC complexes. Dr. P.J.M. van Kan is acknowledged for critically reading and discussing this manuscript. This research was supported by the Dutch Foundations for Chemical Research (SON) and for Biophysics (SvB), financed by the Netherlands Organization for Scientific Research (NWO). J.P.D. was supported by a fellowship from the Royal Netherlands Academy of Arts and Sciences (KNAW). W.N. acknowledges financial support from the Royal Society, U.K. (Leverhulme William and Mary Research Fellowship).

References

1 Michel, H. and Deisenhofer, J. (1988) Biochemistry 27, 1–7.
2 Diner, B.A. and Petrouleas, V. (1987) Biochim Biophys. Acta 895, 107–125.
3 Moënne-Loccoz, P., Robert, B. and Lutz, M. (1989) Biochemistry 28, 3641–3645.
4 Lubitz, W., Isaacson, R.A., Okamura, M.Y., Abresch, E.C., Plato, M. and Feher, G. (1989) Biochim. Biophys. Acta 977, 227–232.
5 Nabedryk, E., Andrianambinintsoa, S., Berger, G., Leonhard, M., Mäntele, W. and Breton, J. (1990) Biochim. Biophys. Acta 1016, 49–54.
6 Breton, J. (1990) In Perspectives in Photosynthesis (Jortner, J. and Pullman, B., eds.), pp. 23–28, Kluwer, Dordrecht.
7 Van Kan, P.J.M., Otte, S.C.M., Kleinherenbrink, F.A.M., Nieveen, M.C., Aartsma, T.J. and Van Gorkom, H.J. (1990) Biochim. Biophys. Acta 1020, 146–152.
8 Braun, P., Greenberg, B.M. and Scherz, A. (1990) Biochemistry 29, 10376–10387.
9 Tetenkin, V.L., Gulyaev, B.A., Seibert, M. and Rubin, A.B. (1989) FEBS Lett. 250, 459–463.
10 Kobayashi, M, Maeda, H., Watanabe, T., Nakane, H. and Satoh, K. (1990) FEBS Lett. 260, 138–140.
11 Gounaris, K., Chapman, D.J., Booth, P., Crystall, B., Giorgi, L.B., Klug, D.R., Porter, G. and Barber, J. (1990) FEBS Lett. 265, 88–92.
12 Van Leeuwen, P.J., Nieveen, M.C., Van de Meent, E.J., Dekker, J.P. and Van Gorkom, H.J. (1991) Photosynth. Res. 28, 149–153.
13 Dekker, J.P., Bowlby, N.R. and Yocum, C.F. (1989) FEBS Left. 254, 150–154.
14 Van Dorssen, R.J., Breton, J., Plijter, J.J., Satoh, K., Van Gorkom, H.J. and Amesz, J. (1987) Biochim. Biophys. Acta 893, 267–274.
15 Newell, W.R., Van Amerongen, H., Barber, J. and Van Grondelle, R. (1991) Biochim. Biophys. Acta 1057, 232–238.
16 Newell, W.R., Kwa, S.L.S., Van Mourik, F., Van Amerongen, H., Barber, J. and Van Grondelle, R. (1990) in Current Research in Photosynthesis (Baltscheffsky, M., ed.), pp. I.2.279–I.2.282, Kluwer, Dordrecht.
17 Nanba, O. and Satoh, K. (1987) Proc. Natl. Acad. Sci. USA 84, 109–112.
18 Seibert, M., Picorel, R., Rubin, A.B. and Connoly, J.S. (1988) Plant Physiol. 87, 303–306.
19 Lakowicz, J.R. (1983) in Principles of Fluorescence Spectroscopy (Lakowicz, J.R., ed.), pp. 111–153, Plenum Press, New York.
20 Van Gurp, M., Van Ginkel, G. and Levine, Y.K. (1989) Biochim. Biophys. Acta 973, 405–413.
21 Deisenhofer, J., Epp, O., Miki, K., Huber, R. and Michel, H. (1985) Nature 318, 618–624.
22 Satoh, K. and Nakane, H. (1990) in Current Research in Photosynthesis (Baltscheffsky, M., ed.), pp. I.2.271–I.2.275, Kluwer, Dordrecht.
23 Mimuro, M., Yamazaki, I., Itoh, S., Tamai, N. and Satoh, K. (1988) Biochim. Biophys. Acta 933, 478–486.
24 Shuvalov, V.A., Heber, U. and Schreiber, U. (1989) FEBS Lett. 258, 27–31.
25 Vermeglio, A. and Paillotin, G. (1982) Biochim. Biophys. Acta 681, 32–40.
26 Bolt, J.D. and Sauer, K. (1981) Biochim. Biophys. Acta 637, 342–347.
27 Visschers, R.W., Chang, M.C., Van Mourik, F., Parkes-Loach, P.S., Heller, B.A., Loach, P.A. and Van Grondelle, R. (1991) Biochemistry 30, 5734–5742.
28 Tang, D., Jankowiak, R., Seibert, M., Yocum, C.F. and Small, G.J. (1990) J. Phys. Chem. 94, 6519–6522.
29 Goedheer, J.C. (1966) In The Chlorophylls (Vernon, L.P. and Seely, G.R., ed.), pp. 147–184, Academic Press, New York/London.
30 Fragata, M., Norden, B. and Kurucsev, T. (1988) Photochem. Photobiol. 47, 133–143.
31 Breton, J. (1985) Biochim. Biophys. Acta 810, 235–245.
32 Rutherford, A.W. (1985) Biochim. Biophys. Acta 807, 189–201.
33 Van Mieghem, F.J.E., Satoh, K., and Rutherford, A.W. (1991) Biochim. Biophys. Acta 1058, 379–385.
34 Tapie, P., Choquet, Y., Wollman, F.-A., Diner, B. and Breton, J. (1986) Biochim. Biophys. Acta 850, 156–161.
35 Van Dorssen, R.J., Plijter, J.J., Dekker, J.P., Den Ouden, A., Amesz, J. and Van Gorkom, H.J. (1987) Biochim. Biophys. Acta 890, 134–143.
36 Newell, W.R., Van Amerongen, H., Van Grondelle, R., Aalberts, J.W., Drake, A.F., Udvarhelyi, P. and Barber, J. (1988) FEBS Lett. 228, 162–166.
37 Breton, J., Duranton, J. and Satoh, K. (1988) In Photosynthetic Light-Harvesting Systems (Scheer, H. and Schneider, S., eds.), pp. 375–386, W. de Gruyter, Berlin/New York.